*Exp. Theo. NANOTECHNOLOGY* 10 (2026) 1991-2002 https://doi.org/10.56053/10.4.1991

# Effect of anodization voltage on $NO_2$ gas sensing performance of $TiO_2$ and Ag-$TiO_2$ nanotube arrays

*Maysoon F A Alias[1,*], Zainab R. Muslim[1], Zina A. Al Shadidi[2], Bahar M. Aljaf[3], Ali Q. Kadhum[1]*

[1]University of Baghdad, College of Science, Department of Physics, Baghdad, Iraq
[2]Al Ma'moon University College, Department of radiology, Baghdad, Iraq
[3]University of Oldenberg, Sustainable Renewable Energy, Germany
[*)] Email: maysoon.ahmed@sc.uobaghdad.edu.iq

*Received* 25/6/2026, *Received in revised form* 23/8/2026, *Accepted* 10/9/2026, *Published* 15/10/2026

The effects of anodization voltages (50 V and 80 V) on the morphological properties of $TiO_2$ nanotube arrays and their $NO_2$ gas sensing performance are investigated. The thin films are synthesized using the electrochemical anodization method and characterized via energy dispersive X-ray spectroscopy (EDX), atomic force microscope (AFM) and scanning electron microscopy (SEM). The results demonstrated that the nanotubes' length, diameter, and surface roughness are significantly influenced by the anodization voltage, where higher voltage (80 V) led to increase dimensions. Sensing tests revealed that Ag-doping significantly enhances sensitivity compared to pure $TiO_2$ nanotubes. The gas sensing mechanism confirmed that $NO_2$ acts as an oxidizing gas, leading to an increase in the electrical resistance of the n-type $TiO_2$ nanotubes. The maximum sensitivity is achieved at an optimum operating temperature of 200 °C. Furthermore, the Ag-$TiO_2$ sensor exhibited improved response and recovery times, making it a highly efficient candidate for detecting $NO_2$ gas in environmental monitoring applications.

**Keywords:** $TiO_2$ nanotubes; Voltage variation; $NO_2$ gas sensing; Electrochemical anodization; Ag-doped $TiO_2$.

## 1. INTRODUCTION

As molecule detection is indispensable in modern technology, with critical applications spanning environmental monitoring, industrial safety, healthcare, and chemical process control. To address these

needs, various gas sensing technologies have been developed, including catalytic, electrochemical, thermal conductivity, optical, and semiconductor-based sensors. Among these, metal oxide semiconductor (MOS) gas sensors have attracted widespread attention due to their high response values, excellent stability, and cost effectiveness [1-5]. Metal oxides nanocomposites such as lithium oxide, iron oxide, and titanium dioxide ($TiO_2$), are considered fundamental building blocks in advanced devices. Beyond gas sensing, their unique physical and chemical properties including high thermal stability and surface activity make them essential in energy storage systems, such as lithium-ion batteries, where they enhance capacity and conductivity. Recently, research has shifted toward mixed oxide systems and nanocomposites to tailor these properties for specific functionalities, often yielding performance that surpasses single component oxides [6-11]. The morphology and dimensions of these nanostructures play a decisive role in their sensing performance. In particular, tubular-shaped nanostructured titania ($TiO_2$) has emerged as one of the most promising materials for gas sensing devices [12]. The unique architecture of $TiO_2$ nanotubes provides a vast surface area and high porosity, which significantly enhances gas sensitivity and facilitates faster charge transport.

For instance, Regonini et al. [13] have demonstrated that anodization voltage directly influences the morphological properties of $TiO_2$ nanotubes, where higher voltages enhance tube dimensions and porosity.The synthesis and application of metal oxide nanostructures have revolutionized the field of nanotechnology due to their versatile electronic, optical, and chemical properties, serves as critical components in solar cells [14,15], photocatalysis, and advanced gas sensing devices. The effectiveness of these oxides is fundamentally tied to their architectural dimensions and crystal phases, which are precisely tuned during the preparation process [16-23]. Despite their potential, pure $TiO_2$ nanostructures face challenges, such as limited conductance in air and the need for improving recovery durations. To overcome these limitations and extend their application in chemical sensing, researchers are exploring structural modifications and the incorporation of noble metals. The aim of this work is to systematically study the sensing properties and performance of pure $TiO_2$ and Ag-$TiO_2$ nanostructured materials prepared at different anodization voltages (50V and 80V) to evaluate the synergistic effects of silver loading and morphological tuning.

## 2. EXPERIMENTAL

### *2.1 Materials*

The materials used in the preparation of $TiO_2$ nanotubes are listed in Table 1.

**Table 1** Chemicals and materials used in process.

| Item | Material | Original | Specification |
|---|---|---|---|
| 1 | Ti Foil | Alfa Aesar A Johnson Matthey company (China) | 99.7% ; thickness 0.25mm |
| 2 | Pt Foil | Sigma Aldrich Company, (Germany) | 99.7% ; thickness 0.25mm |
| 3 | $NH_4F$ | BDH Chemicals Ltd pool (England) | 99.5% |
| 4 | Ethylene Glycol | Sigma Aldrich, (Germany) | 99.8% |
| 5 | $N_2$ | | |
| 6 | Ethanol | (China) | 99.7% pure |
| 7 | Deionized Water | Utilities Lab University of (Baghdad) | Conductivity 10 µm/cm |
| 8 | electric liquid tape | scotch (USA) | |
| 9 | Silver Nitrate | SHAMRAN company (Iran) | 99.9% |
| 10 | Sulfuric Acid ($H_2SO_4$) | (GCC) (UK) | 98% |
| 11 | $NO_2$ gas | | |

2.1 *$TiO_2$ nanotube preparation*

In the electrochemical process, Ti foil represents the anode while, the platinum serves as the cathode. Prior to the anodizing procedure, Ti foils with dimensions of (20×20×0.25) $mm^3$ are degreased by sonication in deionized (DI) water with soap and then with ethanol, each for 15 min. Finally, the Ti foils are rinsed with DI water and dried with $N_2$ After drying the backside of Ti foil is covered by electric liquid tape. The surface area exposed to the electrolyte is about 2.0 $cm^2$. The cell electrolyte is (0.5wt %) of $NH_4F$ in ethylene glycol (95.5 wt%) with (4wt %) DI water, the electrodes are hung on cell cover and immersed in the electrolyte.

The separation between the two electrodes is kept at 3.0 cm in all the experiments. Anodization is carried out for 1hr at two voltages (50and 80) V, in each case the voltage is held constant for 1hr. After the end of anodization, the samples are cleaned with distilled water to remove the anodization ions from the anodization solutions, and dried using $N_2$. The experiments are performed at room temperature.

2.2 *Ag doped $TiO_2$ nanotube*

$TiO_2$ nanotubes prepared for different voltages (50 and 80) V electro- deposition of silver is carried out by mixing (0.1 M sulfuric acid) with (10 mM silver nitrate). The nanotubes are

dipped in the solution mentioned before. All samples are cleaned with DI ionized water then exerted to $N_2$ gas before the metal deposition measurements.

2.3 *Sensor Testing*

Gas sensitive characteristics of $TiO_2$ nanotubes and Ag-$TiO_2$ nanotubes for $NO_2$ gas at low concentrations (10-40) ppm, the method and procedure of sensor response is determined, under the condition that the sensor is under different temperature, (see Figureure 1). The following procedures used in gas sensing are listed below:

- The test chamber is opened and the sensor placed inside it, the necessary electrical connections between the pin feed through and the sensor spring loaded pins and Digital multi meter are made, the test chamber is closed.
- Rotary pump is switched on to evacuate the test chamber to approximately 50 mbar.
- Heat mantle is used for boiling $NO_2$ vapor gas at 21.2 °C.
- After that, needle valves is used to control the flow rate of the carrier and vapor of $NO_2$.
- The vapor of $NO_2$ in mixing chamber is allowed to flow to the test chamber by opening the two-way valve.
- The measurement of the current variation for the sensor for the known concentration of test gas, observed by the PC interfaced digital multi meter.
- After the measurement, the needle valve of the vapor of $NO_2$ is closed to allow the sensor to recover to the base line current $I_0$.
- The above measurements are repeated for different temperatures (50, 100, 150, 200, 250, 300) °C and different concentrations (10, 20, 30, 40) ppm of the vapor. The volume of the chamber= *(*250*)* mL and the sensitivity is:

$$Sensitivity = (R_{gas} - R_{air}) / R_{air} \times 100\% \quad (1)$$

where $R_{gas}$ is resistance of the film in gas and $R_{air}$ is resistance of the film in air.

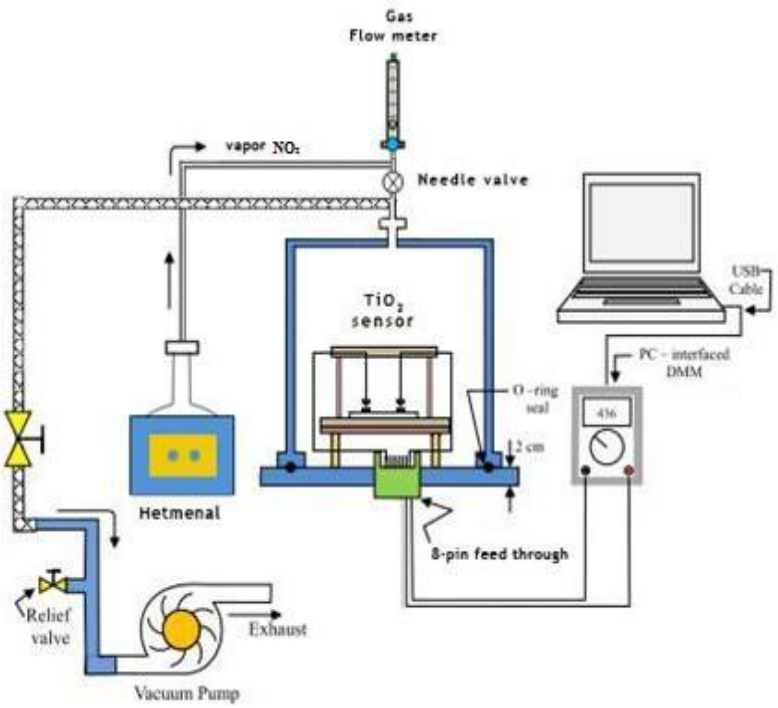


**Figure 1** Gas sensor set up**.**

## 3. RESULTS AND DISCUSSION

### *3.1 Compositional*

The energy dispersive X-ray spectroscopy (EDX) study of $TiO_2$ nanotubes synthesized for anodization potentials of 50 and 80 V is displayed in Figures 2 and 3 respectively. The titanium nano tubes (TNTs) are mostly composed of titanium and oxygen, with trace amounts of other components. The ratio of Ti to O is remarkably close to 1:2.

It is observed that the intensity of the oxygen peaks increased significantly when the anodization voltage is raised from 50V to 80V. This increment in intensity is attributed to the increased thickness of the oxide layer and the growth of longer nanotubes at higher voltages, which led to a higher concentration of oxygen within the scanned area. Regarding the additional peaks observed in the spectra, the presence of carbon or fluorine at a relatively high ratio can be attributed to the residual electrolyte ions or the carbon tape used during sample preparation. Furthermore, a comparative analysis with previous studies [6] indicated that the observed atomic percentages are in good agreement with the stoichiometric requirements for anatase $TiO_2$ structures.

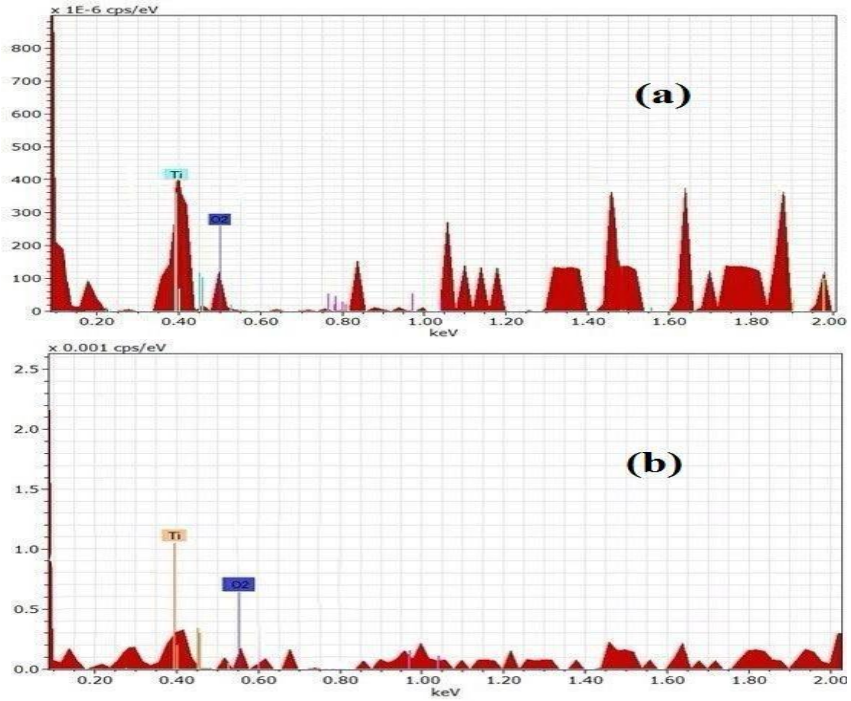


**Figure 2** EDX image of TNT's prepared via anodizing at (a) 50 V and (b) 80V.

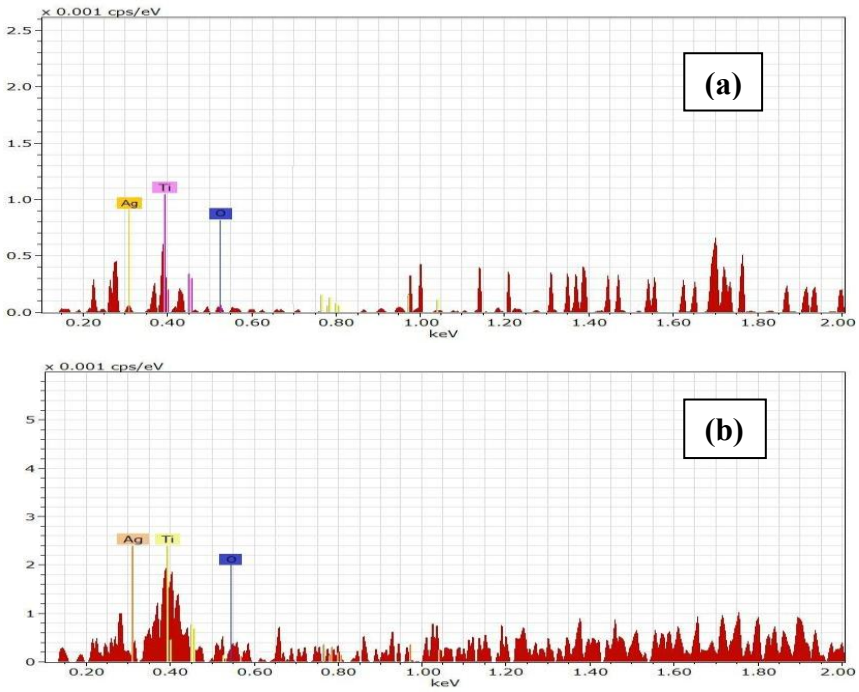


**Figure 3** EDX analysis for the Ag-$TiO_2$ nanotubes synthesized at an anodization potential of (a) 50 V and (b) 80 V.

### *3.2 Morphological properties*

The surface morphology of $TiO_2$ nanotube as observed from the AFM micrographs proved that the grains are uniformly distributed for 2D and 3D views with individual grains extending upwards as shown in Figures 4-7.

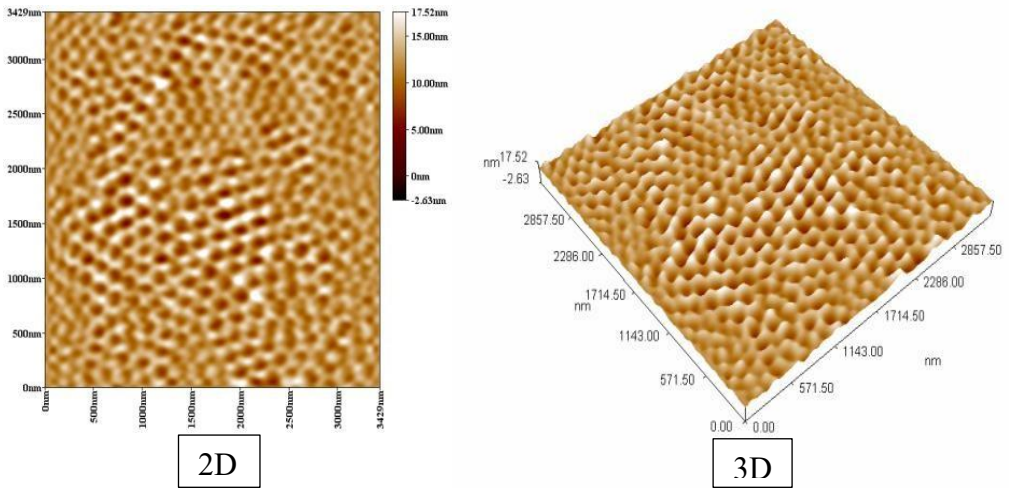


**Figure 4** 2D and 3D AFM images of TNT' synthesized via anodizing at 50 V.

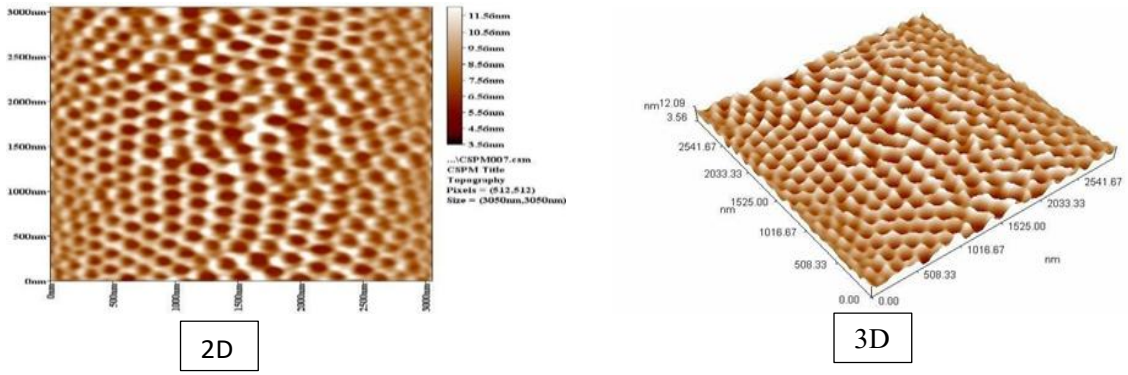


**Figure 5** 2D and 3D AFM images of TNT's synthesized via anodizing at 80 V.

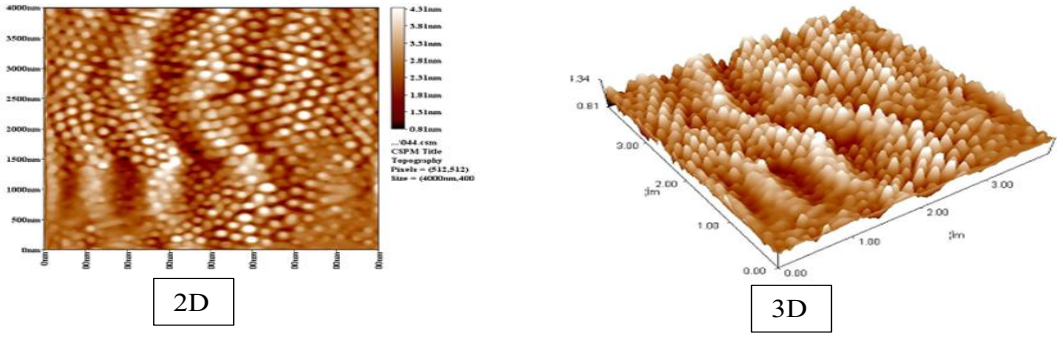


**Figure 6** 2D and 3D AFM images of Ag-$TiO_2$ prepared via anodizing at 50 V.

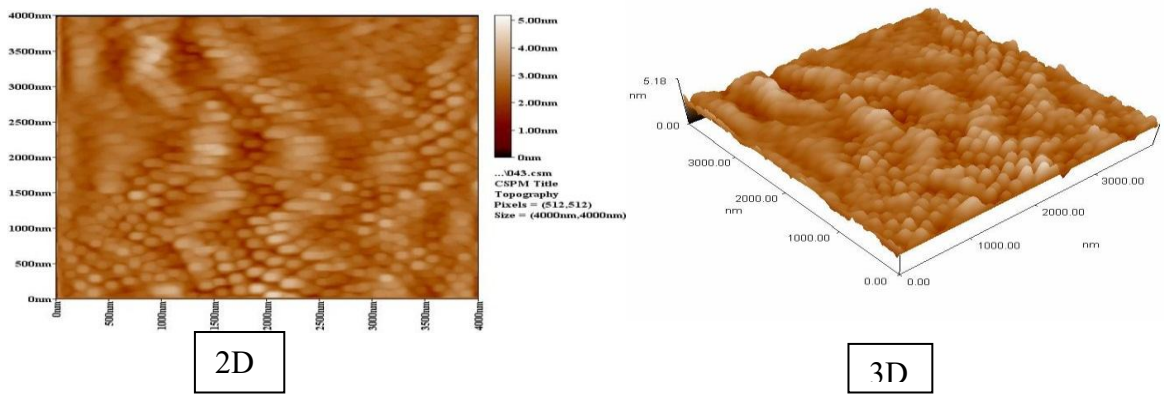


**Figure 7** 2D and 3D AFM images of Ag-$TiO_2$ prepared via anodizing at 80 V.

Images demonstrate how the anodization voltage affects the film surface roughness. It is evident that the surface roughness changes quickly as the tubes start to form, and that, for anodization voltages up to 40, there is very little change in surface roughness. One can observe that the pore depth and the wall thickness decreased as the voltage increased. In contrast to Figures 4 and 5a higher roughness for Ag doped TNTS showed that particle distribution influences porosity, which in turn impacts gas flow and transport parameters (Figures 6 and 7). Due to the ensuing morphology and surface chemistry, the sensitivity of the sensors appears to be significantly influenced by the sensing performance as a result of voltage variation, Ag metal deposition, and tube length and diameter.

According to the results of SEM images Figures 8 and 9, Tables 2 and 3 displayed how the anodizing potential affected the TNT's and Ag-$TiO_2$ dimensions, it showed that Tube diameter increased with anodization voltage, while tube length also increased. Figures 10 and 11 display the SEM images for Ag -$TiO_2$ samples generated at 50V and 80V voltages. At 80 V the nanotubes are longer and more uniform, giving higher surface area. At 50 V the structure is shorter and less ordered i.e. higher voltage produces longer, more ordered nanotubes with larger surface area.

**Table 2** Anodizing potential affects the TNT's dimensions (diameter and length).

| Anodizing potential (V) | Tube diameter (nm) | Tube length (μm) |
|---|---|---|
| 50 | ~50-80 | -3 |
| 80 | ~100-150 | 4-7 |

.

**Table 3** Anodizing potential affects the Ag/TNT's dimensions (diameter and length).

| Anodizing potential (V) | Tube diameter (nm) | Tube length (μm) |
|---|---|---|
| 50 | ~50-100 | 1-2 |
| 80 | ~100-150 | 5-8 |

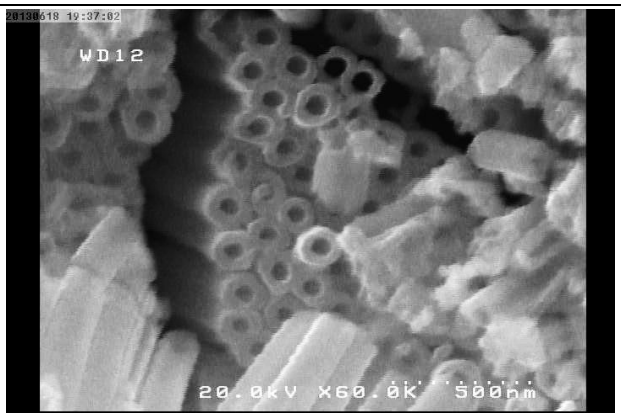


**Figure 8** SEM images of TNT's prepared at 50V.

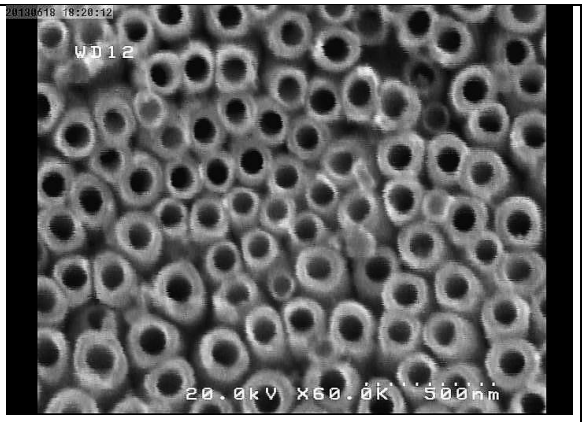


**Figure 9** SEM images of TNT's prepared at 80V.

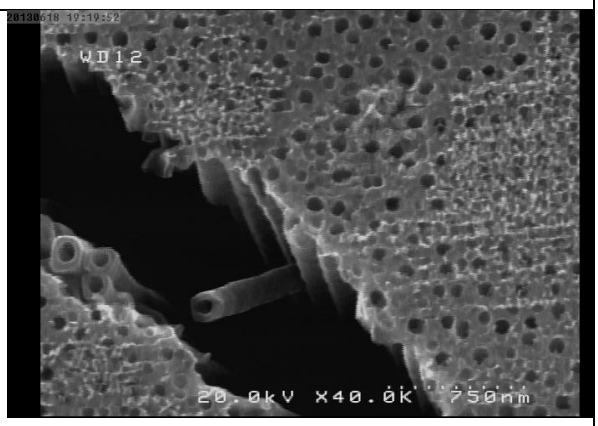


**Figure 10** SEM images of Ag/$TiO_2$ prepared at 50V

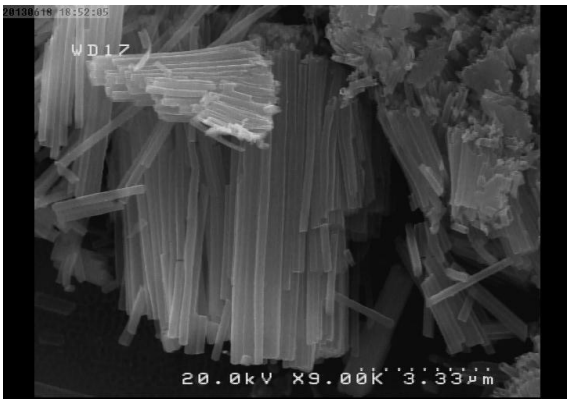


**Figure 11** SEM images of Ag/$TiO_2$ prepared at 80V

*3.3 Gas sensing*

The gas sensing mechanism of $TiO_2$ nanotubes is primarily based on the change in electrical resistance resulting from the chemical interaction between gas molecules and the sensor surface. Since $TiO_2$ is an n-type semiconductor, its majority charge carriers are electrons. When the sensor is exposed to $NO_2$ (an oxidizing gas), the $NO_2$ molecules act as electron acceptors, capturing electrons from the conduction band of the $TiO_2$. This chemisorption process led to an expansion of the electron depletion layer on the nanotube surface, which results in a decrease in the concentration of free electrons and, consequently, an increase in electrical resistance as shown in Figures 12 and 13. This behavior is consistent with the experimental response curves observed in this study, where resistance increases upon exposure to $NO_2$ gas and returns to its baseline value when the gas is removed [24].

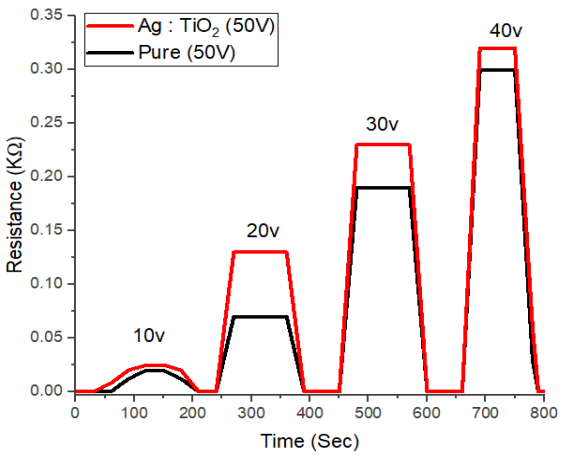


**Figure 12** Relation between resistivity and time working at 50V for pure $TiO_2$ nanotubes.

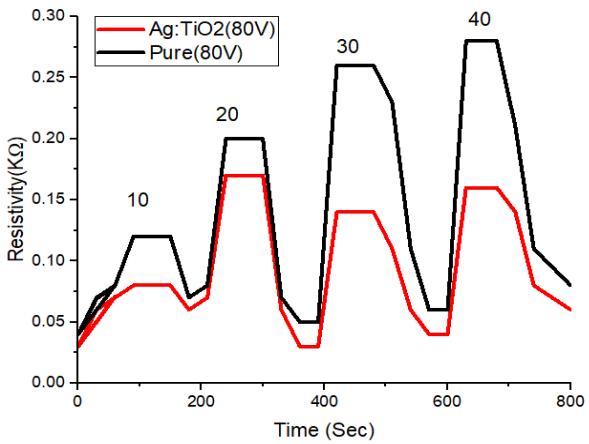


**Figure 13** Relation between resistivity and time at 80V for pure $TiO_2$ and Ag-$TiO_2$ nanotubes.

Figures 14 and 15 illustrate the gas sensing sensitivity of pure TNTS and Ag-$TiO_2$ nanotubes synthesized at 50V and 80V, respectively. It is observed that the sensitivity of the samples produced at 80V is significantly higher than those produced at 50V. This enhanced sensitivity is attributed to the high surface to volume ratio provided by longer and uniform nanotubes and due to chemisorption of $NO_2$ molecules onto the $TiO_2$ surface. The results showed for all samples that the sensitivity increased with temperature, reaching its peak at 200 °C, followed by a decline in the range of 250 to 300 °C, except for pure TNTS at 50 V, the peak is at 250°C. This reduction at higher temperatures can be explained by the increased molecular mobility and gas diffusion, which, despite accelerating the dissociation rate on the sensor surface, eventually leads to a decrease in the overall gas absorption efficiency. At the optimal operating temperature of 250 °C and a concentration of 40 ppm $NO_2$, the Ag-$TiO_2$ sensor exhibited a rapid response time of 35 s and a recovery time of 75 s. In contrast, the pure $TiO_2$ nanotubes showed a slower response, with 95 s and of 180 s. The significant reduction in response and recovery times for the doped samples confirms the effective catalytic role of Ag nanoparticles in accelerating the adsorption-desorption kinetics of $NO_2$ molecules on the $TiO_2$ surface.

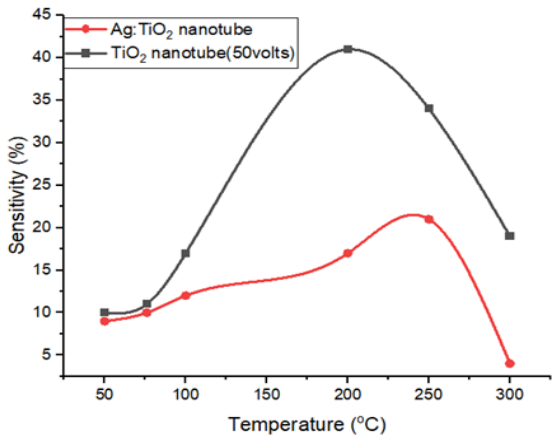


**Figure 14** Sensitivity and working temperature for pure $TiO_2$ and Ag-$TiO_2$ at 50V.

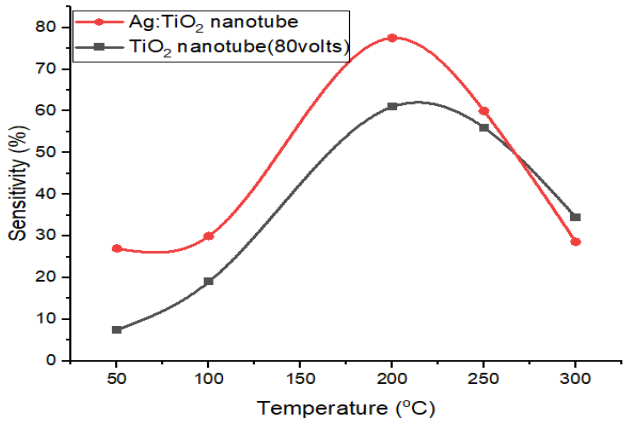


**Figure 15** Sensitivity and working temperature for pure $TiO_2$ and Ag-$TiO_2$ at 80V

## 4. CONCLUSIONS

$TiO_2$ and Ag-doped $TiO_2$ nanotube arrays were successfully synthesized via electrochemical anodization at different voltages (50V and 80V). Gas sensing measurements toward $NO_2$ revealed that the Ag-doped $TiO_2$ sensor fabricated at 80V exhibited the highest sensitivity and faster response/recovery times compared to pure $TiO_2$. The gas sensing mechanism demonstrated that $NO_2$ behaves as an oxidizing gas, causing an increase in the electrical resistance of the n-type $TiO_2$ nanotubes upon exposure. The optimum operating temperature for the fabricated sensors was found to be 200 °C for pure $TiO_2$ and Ag-$TiO_2$ at both anodization voltages, except for Ag-$TiO_2$ at 50V was 250 °C.

## References

[1] R. S. Mahmood, et al., Journal of Mechanical Behavior of Materials, 34 (2025) 1. https://doi.org/10.1515/jmbm-2025-0040
[2] R.Fukuhara,A.Nasu, S.Inasawa, Langmuir 40 (2024)224242432. https://doi.org/10.1021/acs.langmuir.4c03285
[3] Ebtesam F. Khanjer, Ban abul Al-Razak, Mustafa S.Srayyih, Mohammed A. Mohammed, Ameerah Ab. Al-Sadooni, Experimental and Theoretical NANOTECHNOLOGY, 9 (2025) 385 https://doi.org/10.56053/9.S.385
[4] A. Kadhum, Z.R. Muslim, H.I. Jaffer, Acta Physica Polonica A 5 (2019) 135. 10.12693/APhysPolA.135.11367
[5] H.A. Abdulrahman, M.F.A.Alias, Iraqi Journal Sciences 62(2021) 3858. https://doi.org/10.24996/ijs.2021.62.11.7
[6] Zainab Shaheed Kadhim, Haider Y.Hammod, Experimental and Theoretical NANOTECHNOLOGY, 9 (2025) 395 https://doi.org/10.56053/9.S.395
[7] Sadeer M. Majeed, Jaafar M.Mousa, S. Ibraheim Hussein,N. Abbas Ali, A. Shawqi Khalil, Z. Raheem Muslam, AIP Conf. Proc. 3229, (2024) 070017 10.1063/5.0236844
[8] Sadeer M. Majeed, Jaafar M. Mousa, Experimental and Theoretical NANOTECHNOLOGY, 9 (2025) 405 https://doi.org/10.56053/9.S.405
[9] G. Kudur, J. Bhavana R. Praveen Naik, Progress Nano-Hybrid Smart Coatings for Aerospace Applications (2024) 267. https://doi.org/10.1021/bk-2024-1469.Ch012

[10] N. Hasan, Experimental and Theoretical NANOTECHNOLOGY, 9 (2025) 415 https://doi.org/10.56053/9.S.415
[11] Israa Abdulqasim Mohammed Ali, Wafaa Hikmat Wadee, Kamal Mohammed Abood, Experimental and Theoretical NANOTECHNOLOGY, 9 (2025) 423 https://doi.org/10.56053/9.S.423
[12] Marwa Sulaiman, Enas Muhi Hadi, Experimental and Theoretical NANOTECHNOLOGY, 9 (2025) 431 https://doi.org/10.56053/9.S.431
[13] Mohammed J. AlSultani, Maysoon F. Alias, Karbala International Journal of Modern Science 10 (2024)350 10.33640/2405-609X.4473
[14] M.J. AlSultani, M. F. A. Alias, Experiential Theoretical Nanotechnology 9(2025)103. https://doi.org/10.56053/9.S.103
[15] Rana A. Anaee, Rana A. Anaee, Marwa A. Abbas, Saja A. Abdul Maged, Shaimaa A. Naser, Sinan S. Hamdi, Hussain M. Yousif, Nabil J. AL-Bahnam, Tamara A. Anai, Experimental and Theoretical NANOTECHNOLOGY, 9 (2025) 449 https://doi.org/10.56053/9.S.449
[16] Fu, Y., Chi, H., Tu, N., Mao, J., Li, J., Ye, Z., Zhu, L.,Jiang, J.ACS Sensors 11(2026)1496. https://doi.org/10.1021/acssensors.5c03826
[17] Al Shadidi, Z.A., Suhail, M.H., Falih, A.K., Muslim, Z.R., Mutlak, F.A.H., Journal of Optics 54 ( 2025) 111198 10.1007/s12596-025-02660-6
[18] F. Boudou et al., Experimental and Theoretical NANOTECHNOLOGY, 10 (2026) 1411. https://doi.org/10.56053/10.3.1411
[19] R. Fouad and Z. Raheem, Journal of Physics: Conference, 1879 3(2021).032066 10.1088/1742-6596/1879/3/032066
[20] A. Rahim, M. Al Nuaimi, Experimental and Theoretical NANOTECHNOLOGY, 10 (2026) 1187. https://doi.org/10.56053/10.3.1187
[21] Z.R. Muslim, A.Q. Kadhum, Journal of Conference Series 1591(2020)012005 10.1088/1742-6596/1591/1/012005
[22] T. Kashyap, R. Bortamuly, L. Elias, M. R. Das, D. Mahanta, P. Saikia, ACS Applied Nano Materials 7 (2024) 4667 https://doi.org/10.1021/acsanm.3c04601
[23] A. Rahim, M. Al Nuaimi, Experimental and Theoretical NANOTECHNOLOGY, 10 (2026) 1379. https://doi.org/10.56053/10.3.1379
[24] J. Haiquan Wang, Y. Cai, J. Zhao, Z. Gao, Y.Yan Song, ACS Sensors 9 (2024)1644. https://doi.org/10.1021/acssensors.4c00137

© 2026 The Authors. Published by LPCMA (https://etnano.com). This article is an open access article distributed under the terms and conditions of the Creative Commons Attribution license (http://creativecommons.org/licenses/by/4.0/).